Microfluid Nanofluid (2014) 16:779–785
DOI 10.1007/s10404-013-1270-1

SHORT COMMUNICATION

A general condition for spontaneous capillary flow in uniform cross-section microchannels

Jean Berthier · Kenneth A. Brakke · Erwin Berthier

Received: 19 February 2013 / Accepted: 13 October 2013 / Published online: 6 November 2013

Abstract Spontaneous capillary flow (SCF) is a powerful method for moving fluids at the microscale. In modern biotechnology, composite channels—sometimes open—are increasingly used. The ability to predict the occurrence of a SCF is a necessity. In this work, using the Gibbs free energy, we derive a general condition for the establishment of SCF in any composite microchannel of constant cross section, i.e., a microchannel comprising different wall materials and even open parts. It is shown that SCF occurs when the Cassie angle is smaller than $\pi/2$ ($\theta^* < \pi/2$). For a homogeneous confined channel, this relation collapses to the well-known hydrophilic contact angle $\theta < \pi/2$.

Keywords SCF (spontaneous capillary flow) · Gibbs thermodynamic equation · Cassie law

1 Introduction

In modern biotechnology, composite channels—sometimes partly open or with apertures—are increasingly used and spontaneous capillary flow (SCF) is a convenient method to move fluids in such geometries. Spontaneous capillary flow occurs when a liquid volume is moved spontaneously by the effect of capillary forces—without the help of auxiliary devices such as pumps or syringes. These devices using SCF are especially useful for portable systems, which greatly benefit to be equipment-free. Geometries facilitating the establishment of capillary flows in confined channels have been experimentally and numerically investigated (Juncker 2002; Kitron-Belinkov et al. 2007; Zimmerman et al. 2007, 2008; Chen et al. 2009). A general law for determining the condition for a SCF in composite microchannels is needed. A first approach has been proposed by Berthier and Brakke (2012) for an open channel of uniform cross section. In this paper, we generalize this former approach and present a theoretical model—based on the Gibbs free energy—to derive the condition for SCF in any composite channels of uniform cross section, i.e., microchannels with non-homogeneous walls and partly open to external air, as sketched in the Fig. 1. We show that the condition for SCF is simply that the generalized Cassie angle for the composite surface be smaller than 90°. Let us recall that the generalized Cassie angle θ^* is the average contact angle defined in the appropriate way, i.e.,

$$\cos\theta^* = \sum_i (\cos\theta_i f_i) \tag{1}$$

where θ_i is the Young's contact angle with each component i (including air for the open parts), and f_i the areal fraction of each component i in a cross section of the flow (Fig. 1).

The areal fractions are $f_i = w_i/\left(\sum_i w_i + w_F\right)$ and $f_F = w_F/\left(\sum_i w_i + w_F\right)$

2 Theory

Our starting point is the Gibbs thermodynamic equation (Gibbs 1873)

J. Berthier (✉)
CEA-Leti, 17 Avenue des Martyrs, 38054 Grenoble, France
e-mail: jean.berthier@cea.fr

K. A. Brakke
Mathematics Department, Susquehanna University,
514 University Avenue, Selinsgrove, PA 17870, USA

E. Berthier
Department of Medical Microbiology and Immunology,
University of Wisconsin-Madison, Madison, WI 53705, USA

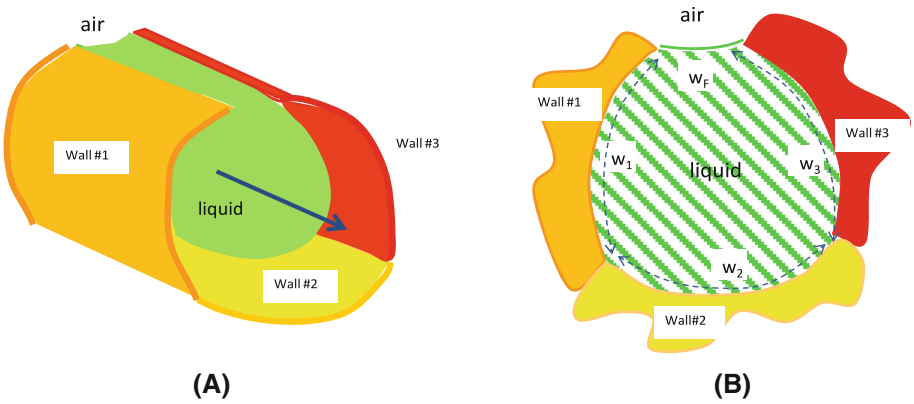

Fig. 1 Cross section of a partly open composite microchannel: the lengths w_i stand for the wetted perimeters and w_F for free perimeter

$$dG = \gamma\, dA - p\, dV - S\, dT \tag{2}$$

where G is the Gibbs free energy, A the liquid surface area, γ the surface tension, V the liquid volume, p the liquid pressure, S the entropy, and T the temperature. Generally, in biotechnology (except for the very special cases where heating is used, such as for polymerase chain reaction PCR), the temperature is kept constant and the last term of (2) vanishes. Assuming a constant temperature, we consider the two following cases: first, the liquid volume is constant, as for a drop with negligible or slow evaporation, and second, increasing volume of liquid. In the first case, (2) reduces to

$$dG = \gamma\, dA \tag{3}$$

The equilibrium position of the droplet is obtained by finding the minimum of the Gibbs free energy. In this case, the minimization of the Gibbs energy is equivalent to the minimization of the liquid surface area.

The second case—that of a SCF—is different: there is not a constant volume of liquid in the system ($dV \neq 0$), and the system evolves in the direction of lower energy. Hence,

$$dG = \gamma\, dA - p\, dV < 0. \tag{4}$$

The morphology of the free interface is such that it evolves to reduce the free energy G. For simplicity, we first consider a single solid wall and air. The liquid (L) is then at the contact of a solid (S) and air (G) as sketched in Fig. 2.

Let us investigate first the upstream conditions. As mentioned earlier in the text, SCF is used as a self-propelling phenomenon and no pump or syringe is present. The upstream condition is most of the time given by the pressure condition of a reservoir of liquid. If we suppose that the reservoir is sufficiently large, as did Bruus (2007), the curvature of its free interface is small and nearly constant, and the upstream pressure is constant and approximately equal to the atmospheric pressure (zero pressure difference).

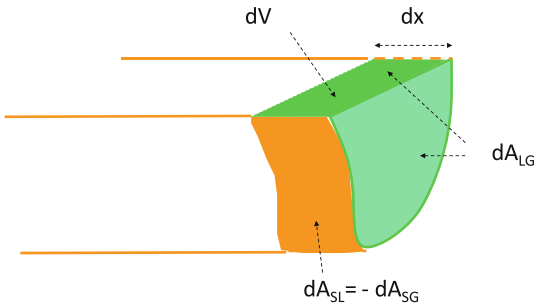

Fig. 2 Sketch of the liquid front advancing along the solid surface by capillarity

Spontaneous capillary flow occurs as long as the pressure at the flow front is smaller than that of the reservoir ($p \sim 0$), i.e.,

$$\sum_i \gamma_i \frac{dA_i}{dV} < 0. \tag{5}$$

where the index i scans all the surfaces A_i (with surface tension γ_i with the liquid). Equation (5) can be written in the form

$$\sum_i \gamma_i \frac{dA_i}{dV} = \gamma_{SG} \frac{dA_{SG}}{dV} + \gamma_{SL} \frac{dA_{SL}}{dV} + \gamma_{LG} \frac{dA_{LG}}{dV} < 0 \tag{6}$$

Considering that any change of A_{SL} is made at the expense of A_{SG}, and using Young's equation $\gamma_{LG} \cos\theta = \gamma_{SG} - \gamma_{SL}$, (6) becomes

$$\frac{dA_{LG}}{dV} < \cos\theta \frac{dA_{SL}}{dV} \tag{7}$$

where θ is the Young's contact angle. In other words, SCF occurs when

$$\frac{dA_{LG}}{dA_{SL}} < \cos\theta. \tag{8}$$

If we denote by w the wetted perimeter, i.e., the length of the contact line between the solid and the liquid in a

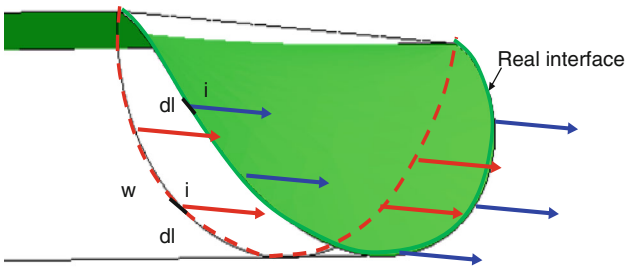

Fig. 3 Sketch of the real interface and the w line

cross section, and w_F the free perimeter, i.e., the length of the front not in contact with the walls in the same cross section, (8) yields the condition (Berthier and Brakke 2012).

$$\frac{w_F}{w} < \cos\,\theta. \tag{9}$$

Condition (9) is a universal criterion for SCF, which is very simple to use and confirmed by numerical and experimental results.

Now, consider the general case of a composite, non-homogeneous channel walls, as in Fig. 1. The condition (6) becomes

$$\sum_i \gamma_i \frac{dA_i}{dV} = \sum_i \left(\gamma_{SG,i}\frac{dA_{SG,i}}{dV} + \gamma_{SL,i}\frac{dA_{SL,i}}{dV}\right) + \gamma_{LG}\frac{dA_{LG}}{dV} < 0 \tag{10}$$

Again, using Young's law and remarking that any change of $A_{SL,i}$ is made at the expense of $A_{SG,i}$ we derive

$$\sum_i \left(-\cos\theta_i \frac{dA_{SL,i}}{dV}\right) + \frac{dA_{LG}}{dV} < 0 \tag{11}$$

where the angles $\theta_i$are the Young's contact angles with each solid. Now, because dV is arbitrary

$$\sum_i \left(-\cos\theta_i\, dA_{SL,i}\right) + dA_{LG} < 0. \tag{12}$$

Even if the real interfaces A are not flat surfaces, there is no loss of generality in writing

$$dA_{SL,i} = dx\, w_i \tag{13}$$

where dx is an infinitesimal progression of the fluid front along the axial direction of the channel (Fig. 2). This property just stems from the fact that the capillary force is identical along any contour left by the triple line (Fig. 3). Indeed,

$$\int_{pw} \gamma\cos\theta\,\vec{i}.\,d\vec{l} = \int_{\text{realinterface}} \gamma\cos\theta\,\vec{i}.\,d\vec{l} \tag{14}$$

On the other hand, the "open" part of the cross section cannot be too large because it would prevent SCF. Then, the interface in the "open" part of the cross section is not much deformed and we can approximate

$$dA_{LG} \approx dx\, w_F. \tag{15}$$

A discussion about this hypothesis will be given later in the text in Sect. 4. It will be shown that the hypothesis underlying (15) is nearly always satisfied, except when the contact angle is very small. Upon substitution of (13) and (15) in (12)

$$\sum_i (-\cos\theta_i\, w_i) + w_F < 0. \tag{16}$$

This latter relation can be rewritten as

$$\sum_i \left(\cos\theta_i \frac{w_i}{L}\right) + \cos\pi\,\frac{w_F}{L} > 0, \tag{17}$$

where $L = \sum_i w_i + w_F$. By analogy, upon introduction of the generalized Cassie angle θ^* defined by

$$\cos\theta^* = \sum_i (\cos\theta_i\, f_i), \tag{18}$$

where f_i is the fractional area of each composite materials ($f_i = w_i/L$,$f_F = w_F/L$), and using the convention that for contact with the air, the contact angle is π, Eq. (16) collapses to the condition

$$\cos\theta^* > 0 \tag{19}$$

or

$$\theta^* = a\cos\left(\sum_i (\cos\theta_i\, f_i)\right) < \frac{\pi}{2}. \tag{20}$$

We find that the condition for SCF in a composite channel is simply that the generalized Cassie angle be smaller than 90°, i.e., the Cassie angle must be lyophilic. It is straightforward to see that the relation (20) collapses to the usual criterion for confined homogeneous channels.

3 Numerical verification

In this section, we present a comparison between the theoretical criterion for SCF given by Eq. (19) and a numerical approach with the Surface Evolver numerical program (Brakke 1992). Note that Surface Evolver does not describe the dynamics of the motion, but iteratively relocates the interface to lower the energy. In the case of SCF, no equilibrium location exists, but we can still use Evolver to predict the direction of motion in SCF (but not the precise dynamics of motion).

Spontaneous capillary flow in two different types of composite channels has been investigated: first, a confined, rectangular microchannel, and second, two different geometries of "open" channels, i.e., channels having a boundary with the surrounding air.

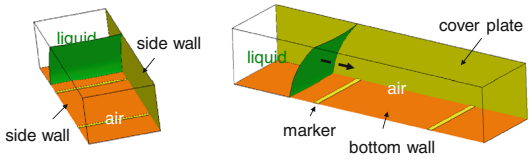

Fig. 4 SCF in a confined microchannel with three different solid walls (bottom, cover, and side walls). *Yellow lines* are markers to check the motion of the interface; some walls have been dematerialized for visualization (color figure online)

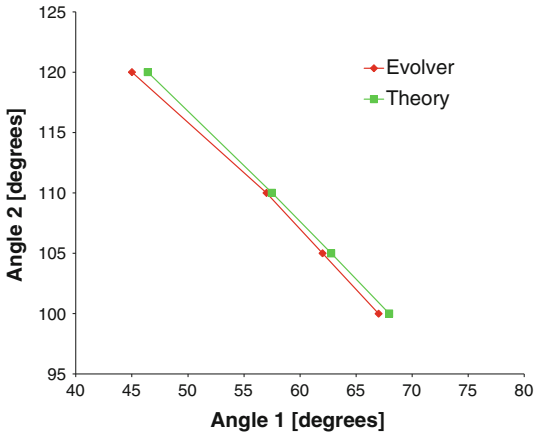

Fig. 5 Comparison between theoretical criterion and Evolver for SCF onset in the case of a rectangular channel with three different contact angles with the liquid. Angles 1 and 2 are, respectively, the top and bottom plate contact angles

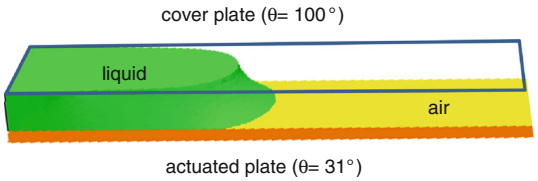

Fig. 6 SCF limit in a two-rail situation

3.1 Composite confined channel

Let us start with the SCF in a confined rectangular microchannel of dimensions 250 × 150 μm with three different solid walls: the top plate has a hydrophilic contact angle of 45° with the liquid while the bottom plate has a contact angle of 120° and the vertical walls a contact angle of 100° (Fig. 4). Substitution in (18) shows that cos $\theta^* \sim 0.02$, or $\theta^* \sim 89.2°$. Using Evolver, we find that it is the onset of SCF. A general comparison between Evolver results and theoretical formula is shown in Fig. 5.

3.2 Composite open channel

Open channels with virtual walls have appeared recently in the literature. In such geometries, the liquid is partly in contact with the surrounding air and partly in contact with different solid walls. Some open channels are simply rails, i.e., a channel wall with air gaps on both sides (Satoh et al. 2005); other open channels are more complex such as open

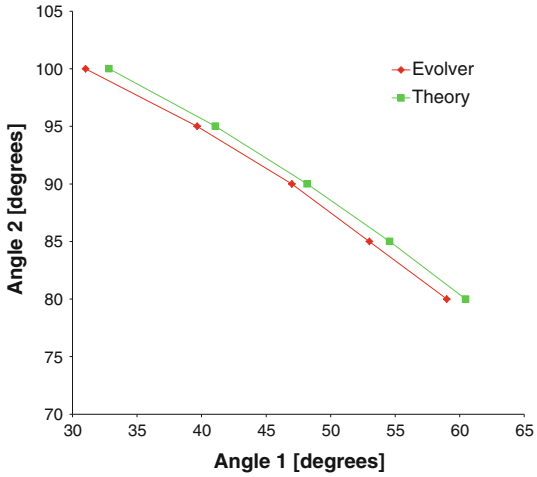

Fig. 7 Comparison between theoretical criterion and Evolver for SCF onset in the case of the two parallel horizontal rails

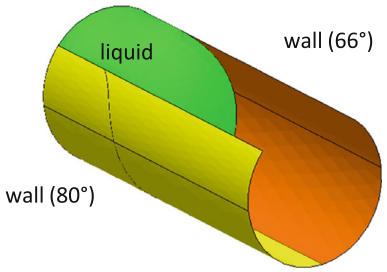

Fig. 8 Composite cylindrical channel

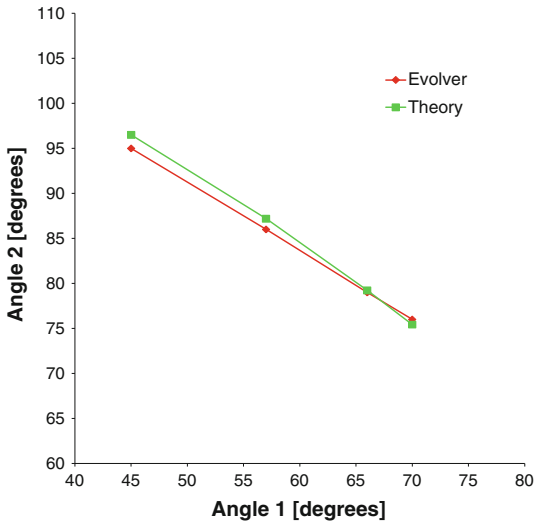

Fig. 9 Comparison between theoretical criterion and Evolver for SCF onset in the case of the composite cylinder

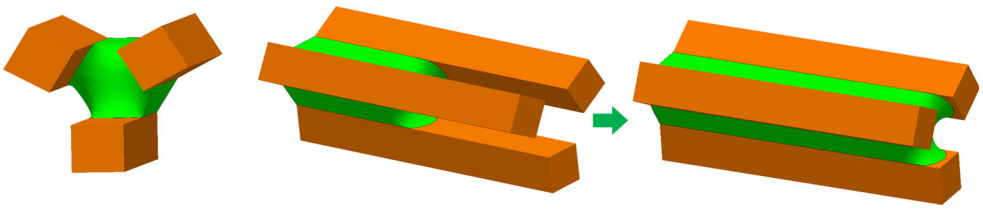

Fig. 10 SCF between three parallel, square rods. *Left* front view of the advancing liquid; middle and *right* perspective view of the advancing SCF

U-grooves with circular apertures in the bottom plate (Berthier et al. 2012).

In the geometry used by Satoh and colleagues, two parallel, horizontal plates—the rails—are used to guide the SCF; the capillary flow is triggered by electrowetting, i.e., the contact angle with the bottom rail is adjusted by a proper level of the electric potential in the electrodes embedded in the rail. The width of the rails is 60 μm and the vertical gap 20 μm. The contact angle with the top plate is 100°, and we find with Evolver that the actuated contact angle with the bottom plate for SCF onset should be 31° (Fig. 6). Substitution of these values in (18) produces the value $\theta^* \sim 89.5°$. A more detailed comparison is shown in Fig. 7, where the SCF limit has been plotted versus the two contact angles with the solid walls. The discrepancy between the two curves—theoretical and numerical—is less than a few degrees.

Finally, we investigate the case of a cylinder partly open, with two different wall materials (Fig. 8). The radius of the cylinder is 200 μm and the width of the opening is 280 μm. Using contact angles of 66° and 80° with the walls, we find $\theta^* \sim 90°$. Again, the value predicted by (18) corresponds to the SCF limit found with Evolver.

A more detailed comparison is shown in Fig. 9, where the SCF limit has been plotted versus the two contact angles with the solid walls. The discrepancy between the two curves—theoretical and numerical—is again less than a few degrees.

4 Discussion

Let us come back on the assumption used for Eq. (15): $dA_{LG} \approx dx\, w_F$. This assumption is linked to a planar top interface and seems to fail when this top interface is distorted. In the following, we consider two examples where the top interface is not planar and assess the effect of the distortion on the SCF condition. It is concluded that relation (15) has a very wide scope of validity.

Consider first the case of three parallel square rods shown in Fig. 10. When the rods are close enough from each other, a reasonably hydrophilic angle is sufficient to observe SCF. When the rods are at a larger distance, small contact angles are needed to establish a SCF. The inter-rod distance corresponding to the limit of SCF has been plotted

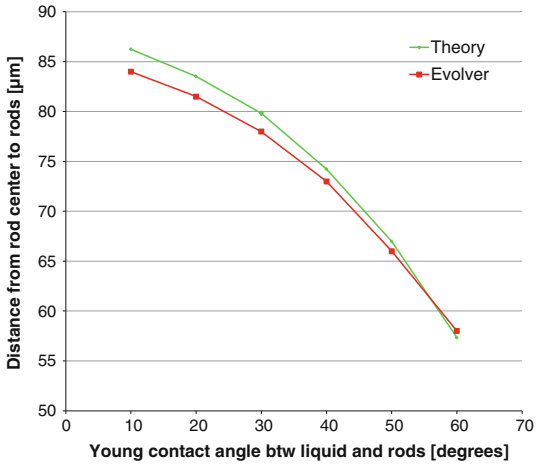

Fig. 11 Comparison between theoretical criterion and Evolver for SCF onset in the case of three parallel rods. The agreement between the two approaches is good for contact angles larger than 30° and a little accurate for contact angles smaller than 30°

versus the contact angles in Fig. 11. The discrepancy between the two curves—theoretical and numerical—is very small for contact angles larger than 30°. Below this value, the relative distance between the two curves is of the order of 5 %. The approximation (15) can still be considered valid.

Another example of distorted interface is that on a suspended V-channel (Fig. 12). When the distance between the two plates at the bottom is very small, the interface is very slanted (Fig. 12a); however, the SCF prediction still corresponds to the results from the Evolver numerical program (Fig. 12c).

5 Experimental verification

At the present time, Eq. (9) has been the basis for a few new developments of open microfluidic systems.

The first developments concern point of care systems (POC) for medicine where blood is directly tested using a finger-pricking device and an open V-groove (Pouteau et al. 2013). The V-groove system has been dimensioned using the SCF condition (9) so that whole blood could flow through the entire device. Fig. 13 shows the V-shaped device and the liquid flowing by capillarity. In this particular case, the advantages of open channels are the

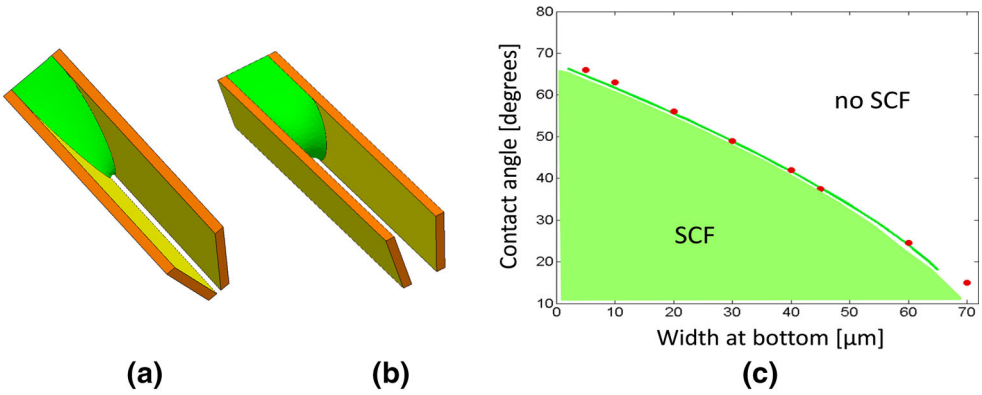

Fig. 12 **a** and **b** suspended SCF in V-shaped channels. **c** Comparison between theoretical formula (9) and Evolver results for the SCF limit in suspended V-shaped channels

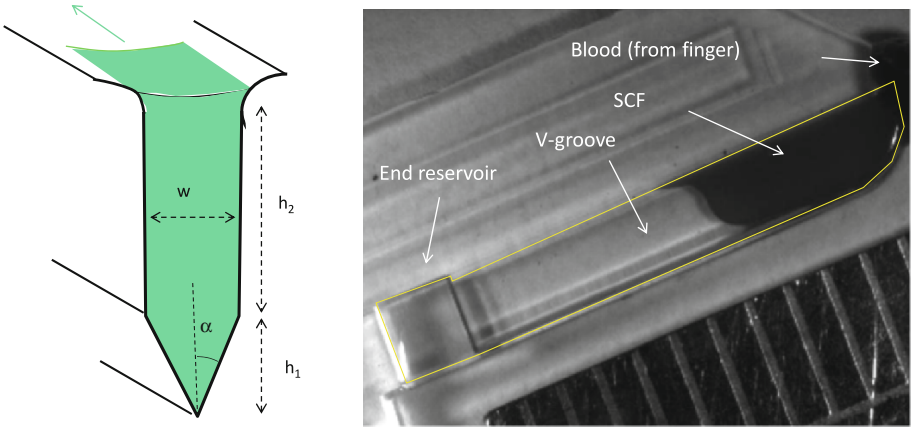

Fig. 13 *Left* cross section of the device; *right* whole blood SCF in the V-groove

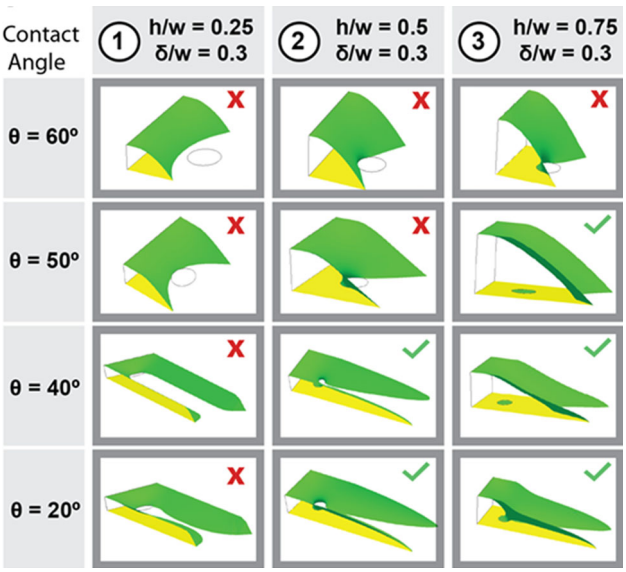

Fig. 14 Capillary flow in a U-shaped channel with holes; *w*, *h,* and δ are, respectively, the channel width, height, and hole diameter; the cases marked with a *red* X do not lead to the filling of the hole, while the cases with a *green* V correspond to the filling of the holes (reprinted with permission from Casavant et al. 2013) (color figure online)

simplicity of fabrication on one hand and on the other hand, the capillary pumping that does not require micropumps—and automatic degasing—so that no air bubble is trapped in the flow.

Another development based on the principle stated in this text concerns the fabrication of µDOTS for cell biology (Casavant et al. 2013). In this application, matrices of suspended collagen membranes have been placed by a SCF in a U-channel passing over holes (Fig. 14). Three possibilities exist, they are follows: (1) the capillary flow is blocked by the holes, (2) it flows around the holes, i.e., the holes are not covered, and (3) the holes are covered, i.e., the SCF is general. Equation (9)—the simplified form of Eq. (19)—is used to determine the geometry corresponding to the required configuration (3).

6 Conclusion

Composite channels with walls of different nature, and sometimes with virtual walls, i.e., open boundaries, are increasingly used in modern biotechnology. In such designs, capillarity is used to move the fluid through the

system. In particular, spontaneous capillary flow (SCF) is especially useful for portable systems, which greatly benefit to be equipment-free.

In order to be able to correctly design such systems, the ability to predict the occurrence of SCF is a necessity. A criterion for the establishment of SCF in such composite channels has been derived in this work. This criterion is very simple: the corresponding generalized Cassie angle must be smaller than 90°. For confined microchannels, the result is straightforward since the capillary line force is the product of the surface tension by the cosine of the contact angle. It is interesting to see that the result is also valid for open channels where a boundary of the fluid flow directly contacts the surrounding air.

References

Berthier J, Brakke K (2012) The physics of microdrops. Scrivener-Wiley publishing. doi:10.1002/9781118401323

Berthier E, Theberge A Casavant B, Chunjun Guo Wang C, Beebe D, Keller N (2012) Suspended microfluidics: an open and user-friendly technology platform for high-throughput metabolic studies, Proceedings of the 2012 MicroTas Conference, Okinawa, Japan, October 28-November 1, 2012

Brakke K (1992) The surface evolver. Exp Math 1(2):141–165

Bruus H (2007) Theoretical microfluidics. Oxford University Press, Oxford

Casavant BP, Berthier E, Theberge AB, Berthier J, Montanez-Sauri SI, Bishel LL, Brakke KA, Hedman CJ, Bushman W, Keller NP, Beebe DJ (2013) Suspended microfluidics. PNAS 110(25):10111–10116

Chen Y, Melvin LS, Rodriguez S, Bell D, Weislogel MM (2009) Capillary driven flow in microscale surface structures. Microelectron Eng 86:1317–1320

Gibbs JW (1873) A method of geometrical representation of the thermodynamic properties of substances by means of surfaces. Trans Conn Acad Arts Sci 2:382–404

Juncker D (2002) Capillary microfluidic systems for bio/chemistry, PhD thesis at the University of Neuchatel, Switzerland, May 8, 2002

Kitron-Belinkov M, Marmur A, Trabold T, Dadheech GV (2007) Groovy-drops: effect of groove curvature on spontaneous capillary flow. Langmuir 23:8406–8410

Pouteau P, Berthier J, Poher V, Dispositif de prélèvement d'un échantillon de liquide par capillarité et procédé d'analyse associé. French Patent, March 7, 2013, n° 13 52050

Satoh W, Hosono H, Suzuki H (2005) On-chip microfluidic transport and mixing using electrowetting and incorporation of sensing functions. Anal Chem 77:6857–6863

Zimmerman M, Schmid H, Hunziker P, Delamarche E (2007) Capillary pumps for autonomous capillary systems. Lab Chip 7:119–125

Zimmerman M, Hunziker P, Delamarche E (2008) Valves for autonomous capillary systems. Microfluid Nanofluidics 5(3):395–402